The Journal of Veterinary Medical Science

FULL PAPER

Pathology

# Effect of a single point mutation on equine herpes virus 9 (EHV-9) neuropathogenicity after intranasal inoculation in a hamster model

**Asmaa G. SALEH[1,2], Shehata I. ANWAR[3], Osama M. ABAS[4,5], Hoda A. ABD-ELLATIEFF [1,6], Mohamed NASR[2], Ibrahim SALEH[7], Hideto FUKUSHI[4] and Tokuma YANAI[1]***

[1]Laboratory of Veterinary Pathology, Faculty of Applied Biological Sciences, Gifu University, 1-1 Yanagido, Gifu 501-1193, Japan
[2]Department of Animal Medicine, Faculty of Veterinary Medicine, Damanhour University, El-Beheira, Egypt
[3]Department of Pathology, Faculty of Veterinary Medicine, Beni-Suef University, Beni-Suef, 62511, Egypt
[4]Laboratory of Veterinary Microbiology, Faculty of Applied Biological Sciences, Gifu University, 1-1 Yanagido, Gifu 501-1193, Japan
[5]Department of Animal Medicine, Faculty of Veterinary Medicine, Alexandria University, Alexandria, Egypt
[6]Department of Pathology and Parasitology, Faculty of Veterinary Medicine, Damanhour University, El-Beheira, Egypt
[7]Department of Pharmacology and Toxicology, Faculty of Pharmacy, Al-Azhar University, Cairo, Egypt

**ABSTRACT.** This study aimed to investigate the neuropathogenesis of equine herpes virus 9 (EHV-9) by studying the effects of a single point mutation introduced in two different EHV-9 genes. The two EHV-9 mutants, 14R and 19R, were generated carrying a point mutation in two separate EHV-9 genes. These mutants, along with the wild-type EHV-9, were used to infect a hamster model. The EHV-9- and 19R-infected groups showed earlier and more severe clinical signs of infection than the 14R-infected group. The white blood cells (WBCs) count was significantly increased in both EHV-9- and 19R-infected groups compared to the 14R-infected group at the 4th day post infection (DPI). Viremia was also detected earlier in both EHV-9- and 19R-infected groups than 14R-infected group. There were differences in the anterograde transmission pattern of both EHV-9 and 19R compared to 14R inside the brain. Serum TNF-α, IL-6 and IFN-γ levels were significantly increased in both EHV-9- and 19R-infected groups compared to the 14R-infected group. Histopathological and immunohistochemical analyses revealed that the mean group scores for the entire brain were significantly higher in both EHV-9- and 19R- infected groups than 14R-infected group. Collectively, these results confirm that the gene product of Open Reading Frame 19 (ORF19) plays an important role in EHV-9 neuropathogenicity and that the mutation in ORF19 is responsible for the attenuation of EHV-9.

**KEY WORDS:** 14R, 19R, EHV-9, hamster, neuropathogenicity

*J. Vet. Med. Sci.*
79(8): 1426–1436, 2017
doi: 10.1292/jvms.17-0076

Received: 19 February 2017
Accepted: 28 June 2017
Published online in J-STAGE: 15 July 2017

Equine herpes virus type 9 (EHV-9), a neurotropic equine herpes virus, is a new member of the equine herpes viruses. It was first isolated from Thomson's gazelles (*Gazella thomsonii*) that died of fulminant encephalitis in a Japanese zoo [13, 36] and thus named Gazelles herpes virus 1 (GHV-1). GHV-1 is serologically related to EHV-1 and EHV- 4 [13]. However, DNA fingerprints of GHV-1 were different from those of EHV-1 and other equine herpes viruses. GHV-1 shows ~95% sequence similarity with EHV-1 and EHV-8, and 60% for EHV-4 based on glycoprotein G gene nucleotide sequencing and a conserved region of the glycoprotein B gene. As such, GHV-1 has since been renamed EHV-9 [12]. Several previous studies demonstrate that EHV-9 can infect various domestic animals, including horses [30], goats [31], pigs [22], dogs [33], cats [34] and cattle [9] as well as non-human primates [35].

The natural host of EHV-9 has been unclear until now, although previous studies suggest that some members of the Equidae family serve as reservoirs for EHV-9. High seroprevalence (60% of 45 animals) was detected in Burchell's zebras in the Serengeti National Park in Tanzania [4] and in Grevy's zebras, as well as an aborted Persian onager in a zoo [25].

Very little is known on EHV-9 neuropathogenicity. As a method to study the pathogenicity of EHV-9, the virus was passaged

*Correspondence to: Yanai, T.: yanai@gifu-u.ac.jp

**Table 1.** Experimental design for the groups of hamsters

| Inoculated virus | Dose/Route | Nos. of animals euthanized on DPI | | | | |
|---|---|---|---|---|---|---|
| | | 2nd | 3rd | 4th | 5th | Total |
| Control | 50 $\mu l$ MEM–α intranasal | 5 | 5 | 5 | 5 | 20 |
| EHV-9 | 50 $\mu l$ ($1 \times 10^4$ PFU) Intranasal | 5 | 5 | 5 | 5 | 20 |
| 14R | 50 $\mu l$ ($1 \times 10^4$ PFU) Intranasal | 5 | 5 | 5 | 5 | 20 |
| 19R | 50 $\mu l$ ($1 \times 10^4$ PFU) Intranasal | 5 | 5 | 5 | 5 | 20 |

multiple times in non-natural cells to induce an attenuated mutant based on the established method [29]. SP21, a mutant strain of EHV-9, was generated by passaging the original virus 23 times in RK13 cells. Full genome sequencing of SP21 revealed two point mutations in open reading frame 14 (ORF14) (asp230tyr) and open reading frame 19 (ORF19) (stop498leu) (Yamada *et al.* and Guo *et al.*, a manuscript in preparation). As correction of these two mutations in two separate clones is away to detect which gene is mainly responsible for the attenuation of the EHV-9, two clones were produced. The first clone, 14R (at which the mutation in ORF 14 has been repaired while in ORF 19 still have mutation). The second clone, 19R (at which the mutation in ORF 19 has been repaired while in ORF 14 still have mutation) (Guo *et al.*, a manuscript in preparation).

The aim of this study was to investigate the virulence of these two clones separately in a hamster model to identify the mutation responsible for EHV-9 attenuation by monitoring the clinical, immunological and histopathological differences in animals infected with EHV-9, 14R or 19R.

## MATERIALS AND METHODS

### *Viral culture*

The EHV-9 virus was propagated on Fetal Horse Kidney (FHK) cells. Briefly, inocula were prepared by culturing the virus from original EHV-9 seed stocks in cells (P20, 5th passage in MDBK cells). The virus was titrated by plaque forming assay on MDBK cells, and the titer of viral suspension was $1 \times 10^4$ PFU/m*l*. The 14R and 19R mutant clones were generated by homologous recombination, propagated on Fetal Horse Kidney (FHK) cells, titrated by a plaque forming assay on MDBK cells and diluted to $1 \times 10^4$ PFU/m*l* viral suspension.

### *Animals and experimental design*

Eighty 3–4 week-old male Syrian hamsters (*Mesocricetus auratus*) were purchased from SLC Inc. (Hamamatsu, Japan) and acclimatized for two days before inoculation with the virus. Animals were housed in an isolated biohazard cabinet, fed a basal diet of pellets (Oriental MF, Oriental Yeast Co., Tokyo, Japan) and allowed sterilized water *ad libitum*.

The hamsters were randomly divided into four groups of 20 hamsters (Table 1) with each group housed separately to prevent cross-infection. The group 1 served as controls and received 50 $\mu l$ of Minimum Essential Media (MEM-α medium) by intranasal administration, while groups 2–4 received 50 $\mu l$ of MEM-α containing $1 \times 10^4$ PFU of EHV-9, 14R or 19R, respectively, by intranasal administration divided between both nostrils while the animals were under deep anesthesia. Five hamsters from each group were sacrificed at 2nd, 3rd, 4th and 5th DPI.

The study protocols were approved by the Committee of Gifu University Animal Experiments. All animal handling and procedures were carried out in accordance with the appropriate institutional animal care guidelines.

### *Clinical evaluation*

Hamsters were monitored three times daily for 5 DPI for any clinical symptoms of encephalitis and changes in bodyweight gain.

### *Necropsy, collection and sample processing*

Two blood samples were collected directly from the heart of each hamster at different time points before necropsy. The first sample was collected in two separate ethylene diamine tetra acetic acid (EDTA)-coated tubes for hematological analysis and viral DNA extraction, respectively. The second sample was collected without anticoagulant to measure serum concentrations of the inflammatory cytokines, TNF-α, IFN-γ and IL-6.

Complete necropsy was performed on all hamsters immediately after death or euthanasia on 2–5 DPI. Five hamsters from each group were euthanized. Brains were removed and examined for gross lesions and mid-sagittally dissected under aseptic conditions. The left hemisphere was used for DNA extraction to detect viral DNA, and the right subjected to histopathological and immunohistochemical analyses.

### *Hematological evaluation*

Complete blood cell counts including white blood cells (WBCs), red blood cells (RBCs), hemoglobin (HGB), hematocrit (HCT), mean corpuscular volume (MCV), mean corpuscular hemoglobin (MCH), mean corpuscular hemoglobin concentration (MCHC) and platelets (PLT) were performed with EDTA-treated blood collected at specific time points from a non-infected control hamster as well as hamsters infected with EHV-9, 14R or 19R (Monolis Laboratory, Tokyo, Japan) using the Celltac α Automatic Hematology Analyzer (Nihon Kohden, Tokyo, Japan).

### *DNA extraction and viral detection*

*DNA extraction and viral detection from blood*: For each hamster, 50 *µl* of blood was collected directly from the heart in an EDTA-coated tube and used for viral DNA extraction with a DNeasy® Blood and Tissue Kit (Qiagen, Tokyo) according to the manufacturer's instructions. The extracted DNA was stored at −80°C until used for PCR analysis.

*DNA extraction and viral detection from the brain*: Brains were also harvested for analysis. Briefly, each half of the brain was divided into three parts: (i) the anterior part (olfactory bulb), (ii) the middle part (cerebrum) and (iii) the hind part (brain stem), and then, each part of the brain was collected in Eppendorf tubes on ice and homogenized with a sterilized plastic tissue homogenizer. DNA was extracted from each part separately using a DNeasy Blood & Tissue Kit (Qiagen) according to the manufacturer's instructions and stored at −80°C until PCR analysis to assess anterograde transmission of the virus to the brain tissue at different time points.

Two primers targeting the EHV-9 DNA polymerase ORF30 sense 5′-GTCAGGCCCACAAACTTGAT-3′ and ORF30 antisense 5′-ATAGGAGTCTGTGCCGTTGT-3′ were designed using the Snap Gene 2.6 software for use in conventional PCR. The target amplified area is 214 bp amplicon. PCR amplification was performed in a 25-*µl* volume containing 2 *µl* of DNA, 2 *µl* of dNTP, 1 *µl* (10 *µ*M) of each primer, 2.5 *µl* 10X Ex Taq buffer, 0.25 *µl* Ex Taq polymerase (Takara, Kyoto, Japan) and 17.25 *µl* distilled water. The thermocycling conditions were as follows: an initial denaturation of 5 min at 94°C, followed by 35 cycles of amplification for 5 sec at 98°C, 30 sec at 47°C and 45 sec at 72°C and a final extension for 7 min at 72°C. The PCR products were separated in 1.5% agarose gels, stained with ethidium bromide, and visualized and photographed with a gel documentation system.

### *Enzyme-linked immunosorbent assay for the determination of cytokines levels in the serum*

TNF-α, IFN-γ and IL-6 serum levels in infected hamsters were measured at different time points and compared with the corresponding non-infected controls to determine differences between EHV-9, 14R and 19R infected groups. Hamster ELISA kits for TNF-α and IFN-γ were purchased from My Biosource Company (San Diego, CA, U.S.A.). The IL-6 ELISA kit was from CUSABIO Company (San Diego, CA, U.S.A.). Each sample was tested in duplicate with a standard to obtain accurate results and absorbance measured by an iMark Microplate Absorbance Reader (Bio-Rad, Hercules, CA, U.S.A.) using a dual wavelength measurement mode with a 450 nm filter and a 630 nm reference filter for TNF-α and a single wave length at 450 nm filter for IFN-γ and IL-6 as recommended by the kit inserts. Sample concentrations were obtained using a standard curve in Microsoft Excel software 2010 with the following formula:=IFERROR (TREND (A2:A8,B2:B8,B23),"").

### *Histopathology*

Tissue samples were fixed in buffered formalin and embedded in paraffin wax. Three-micron sections were cut with a microtome and stained with hematoxylin and eosin (HE) using standard methods. The anterior/olfactory, cerebrum and brain stem sections were evaluated microscopically for the presence of viral antigen, anatomical localization and severity of histopathological lesions to evaluate the viral-associated histopathological lesions; grades indicated cellular inflammatory infiltration, microglial activation and neuronal degeneration based on previously described grading systems [1, 20, 23]. The grading scale included five scores: 0=no lesions; 1=minimal; 2 =mild; 3=moderate and 4=severe. A mean score and standard deviation were calculated based on at least two readings from separate sections within each defined anatomical region. Mean group histopathological scores and standard deviations for the entire brain were calculated based on the total number of readings at a given time point.

### *Immunohistochemical detection of viral antigens*

Paraffin-embedded brain sections were immunolabeled with EHV-9 rabbit antiserum using the EnVision + System HRP labeled polymer (Dako, Santa Clara, CA, U.S.A.) [2]. The primary antibody was EHV-9 antiserum (1:800), followed by application of a secondary antibody (biotinylated anti-rabbit IgG secondary antibody (Dako) with Liquid DAB Substrate Chromogen System (Dako) used as the chromogen and hematoxylin counterstain as previously described [8]. Tissue sections from confirmed EHV-9-infected hamsters were used as positive control samples, and sera from a non-immunized rabbit and goat were used as a negative control treatment on positive control specimens. Sections were semi-quantitatively evaluated and scored as (−) for negative and (+), (++) and (+++) degrees of positivity.

### *Statistical analysis*

One-way analysis of variance with Tukey Kramer post-hoc testing was performed in GraphPad Prism 5 software (San Diego, CA, U.S.A.) to assess differences in bodyweight gain, hematological evaluation and serum cytokine levels. Student's *t*-testing was used to identify significant differences in histopathology scores and immunohistochemical labeling of the entire brain. Data represent the total number of readings at a given time point. All comparisons were considered significant at $P \leq 0.05$.

## RESULTS

### *Clinical findings*

The rate of infection at each day of the experiment is shown in Table 2. The EHV-9 infected group started to show clinical symptoms at 3rd DPI. One animal died at 4th DPI and two at 5th DPI. Early clinical signs included depression, salivation, nasal discharge, lack of coordination and periodic convulsions, which later developed into lateral recumbency and coma in most animals. Some animals also showed bilateral hemorrhage from the nostrils. In comparison, clinical signs were first detected in the

**Table 2.** The rate of infection at each day of the experiment

| Hamster groups | DPI | | | | | | | | | | | |
|---|---|---|---|---|---|---|---|---|---|---|---|---|
| | 0 day (day of infection) | | 1st DPI | | 2nd DPI | | 3rd DPI | | 4th DPI | | 5th DPI | |
| | 1st 12 hr | 2nd 12 hr | 1st 12 hr | 2nd 12 hr | 1st 12 hr | 2nd 12 hr | 1st 12 hr | 2nd 12 hr | 1st 12 hr | 2nd 12 hr | 1st 12 hr | 2nd 12 hr |
| Control group | 0/20Δ | 0/20 | 0/20 | 0/20 | 0/20 | 0/15 | 0/15 | 0/10 | 0/10 | 0/5 | 0/5 | |
| EHV-9 infected group | 0/20 | 0/20 | 0/20 | 0/20 | 0/20 | 0/15 | 5/15 | 2/10 | 7/10 | 3/4 | 2/2*** | |
| 14R infected group | 0/20 | 0/20 | 0/20 | 0/20 | 0/20 | 0/15 | 0/15 | 0/10 | 0/10 | 0/5 | 1/5 | |
| 19R infected group | 0/20 | 0/20 | 0/20 | 0/20 | 0/20 | 0/15 | 0/15 | 5/10 | 10/10 | 5/5 | 5/5 | |

(*) means number of dead animals. (Δ) number of hamsters showed clinical signs/total number of hamsters.

19R-infected group during the second half of 3rd DPI, but were less severe than EHV-9-infected group as indicated by milder depression and a lack of recumbency and deaths. Further, only one 14R-infected hamster showed clinical symptoms at 5th DPI, which included salivation and slight tremors. All animals were alert, and no recumbency was observed.

*Changes in bodyweight gain*

Both EHV-9- and 19R-infected groups showed a significant reduction in bodyweight gain over 5 DPI compared to control and 14R-infected groups (Fig. 1).

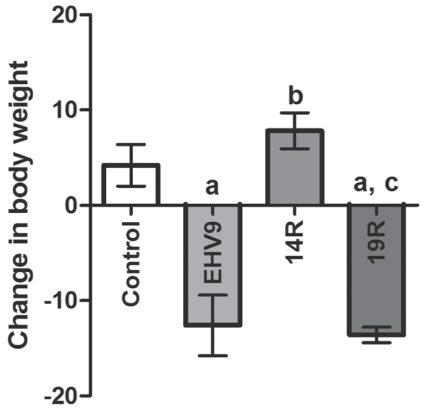


**Fig. 1.** Changes in bodyweight gain. Significant differences were observed in the control (a), EHV-9-infected (b) and 14R-infected (c) groups after 5 DPI. $P \leq 0.05$.

*Hematological evaluation*

Hematological analysis revealed a significant increase in total WBCs in the EHV-9-, 14R- and 19R-infected groups compared to the control group at all time points. Furthermore, a significant increase in total WBCs was noted at 4th DPI in both EHV-9- and 19R-infected groups compared to 14R-infected group (Fig. 2). No other changes were observed when compared to controls.

*PCR for viral DNA detection*

Blood and brain samples were analyzed by PCR for the presence of viral DNA. Notably, EHV-9- and 19R-infected groups became viremic at 3rd DPI, whereas 14R-infected group became viremic at 4th DPI (Table 3). In brain samples, EHV-9 and 19R DNAs were detected throughout the brain in all animals starting by 2nd DPI until the end of the experiment (5th DPI). In comparison, viral DNA was found in the olfactory tissue of two and the cerebral tissue of one 14R-infected animal by 2nd DPI and in the brain stem of all animals by 5th DPI (Table 4).

*Enzyme- linked immunosorbent assay for detection of cytokines levels in the serum*

Viral infection is associated with an increase of pro-inflammatory cytokines in the blood serum. Consistently, serum TNF-α levels were significantly increased in EHV-9-infected animals compared to controls, and 14R- and 19R-infected groups at 3rd DPI, and in both EHV-9- and 19R-infected groups at 4th and 5th DPI (Fig. 3). Similarly, serum IFN-γ levels were significantly higher in both the EHV-9- and 19R-infected animals compared to the 14R-infected group at 2nd DPI, whereas only the EHV-9-infected group had significantly higher serum IFN-γ levels at 3rd DPI. By 4th DPI, both the EHV-9- and 19R-infected groups showed significantly higher levels compared to the 14R-infected group (Fig. 4). Serum IL-6 was significantly increased in all three infected groups at 4th and 5th DPI. Furthermore, a significant increase was also observed in EHV-9-infected animals compared to the 14R-infected group at 4th DPI, and both the EHV-9- and 19R-infected groups by 5 DPI (Fig. 5).

*Gross findings*

No specific gross abnormalities were observed in the organs and tissues of either group at necropsy, except for congestion of the meningeal and cerebral blood vessels.

*Spectrum of virus-associated histopathology*

Various degrees of non-suppurative encephalitis characterized by perivascular cuffing, focal or diffuse gliosis, neuronal degeneration and neuronal loss were observed in all infected animals (Fig. 6). Lesions were predominant in the olfactory bulb and gray matter of the cerebrum.

*Severity of virus-associated central nervous system (CNS) histopathology*

The severity of histopathological lesions in the entire brain gradually increased after inoculation in all infected animals; however, no lesions were detected in the cerebellum. The rostral telencephalon, particularly the rhinencephalon, was the most affected

**Table 3.** PCR analysis for detecting viral DNA in the blood for EHV-9-, 14R- and 19R- infected groups

| DPI | 2nd DPI | | | | | 3rd DPI | | | | | 4th DPI | | | | | 5th DPI | | | | |
|---|---|---|---|---|---|---|---|---|---|---|---|---|---|---|---|---|---|---|---|---|
| Hamster number | 1 | 2 | 3 | 4 | 5 | 1 | 2 | 3 | 4 | 5 | 1 | 2 | 3 | 4 | 5 | 1 | 2 | 3 | 4 | 5 |
| EHV-9 infected group | – | – | – | – | – | – | + | – | + | – | + | + | + | – | – | + | + | * | * | * |
| 14R-infected group | – | – | – | – | – | – | – | – | – | – | – | – | + | – | – | – | + | – | – | – |
| 19R-infected group | – | – | – | – | – | – | – | – | + | – | + | + | – | – | – | + | – | – | – | – |

(+): Positive; (−): Negative. (*): Blood samples from this animal could not be collected, as it was dead before necropsy.

**Table 4.** PCR analysis for detecting viral DNA in various parts of the brain of EHV-9-, 14R- and 19R-infected groups

| DPI | EHV-9 infected group | | | 14R infected group | | | 19R infected group | | |
|---|---|---|---|---|---|---|---|---|---|
| | Anterior part | Middle part | Posterior part | Anterior part | Middle part | Posterior part | Anterior part | Middle part | Posterior part |
| 2nd DPI | + | + | + | – | – | – | + | + | – |
| | + | + | + | + | – | – | + | – | – |
| | + | + | – | – | – | – | + | + | + |
| | + | + | + | – | – | – | + | – | – |
| | + | – | – | + | + | – | + | + | – |
| 3rd DPI | + | + | + | + | + | – | + | + | – |
| | + | + | – | – | – | – | + | + | + |
| | + | + | + | + | – | – | + | + | + |
| | + | – | – | + | + | + | + | + | – |
| | + | + | + | + | – | – | + | + | + |
| 4th DPI | + | + | + | + | + | – | + | + | + |
| | + | + | + | + | + | + | + | + | – |
| | + | + | + | + | – | – | + | + | + |
| | + | + | + | + | + | – | + | + | – |
| | + | + | + | + | – | – | + | + | + |
| 5th DPI | + | + | + | + | + | + | + | + | + |
| | + | + | + | + | + | – | + | + | – |
| | + | + | + | + | + | + | + | + | + |
| | + | + | + | + | + | + | + | + | + |
| | + | + | + | + | + | + | + | + | + |

(+): Positive; (−): Negative.

region independent of the virus subtype. Although no specific anatomical structure of the brain was targeted, scattered regions of inflammation were observed in the olfactory bulbs, cerebrum (including the cingulate gyrus, basal nuclei and pyriform lobes), thalamus (including the hypothalamus, thalamic nuclei, cingulate gyrus, amygdala, fornix, hippocampus and geniculate nuclei), midbrain and rostral medulla.

All EHV-9- or 19R-infected hamsters showed inflammatory changes starting from the 3rd DPI (Table. 5). The degree of encephalitis was mild to moderate, and the inflammatory lesions were restricted to the olfactory bulbs. No other significant differences between the two viruses were observed in this regard. By 4th and 5th DPI, the inflammatory changes spread gradually to the cerebrum, and moderate to severe encephalitic lesions were detected in the olfactory bulbs and the cerebral cortex in both EHV-9- and 19R-infected hamsters. In addition, minimal to slight lesions were observed in the brain stem and medulla oblongata. On the other hand, 14R-infected animals showed no lesions at 3rd DPI, but minimal encephalitis was detected only in one animal at 4th DPI. Two hamsters showed minimal to mild encephalitic changes in the form of a sparse foci of perivascular cuffing in the grey and white matter at 5th DPI (Table 5). The perivascular cuffing was occasionally associated with weak focal or diffuse gliosis. When present, these changes had the same distribution as the encephalitis induced by EHV-9.

Hamsters inoculated with EHV-9 or 19R had significantly higher histopathological scores for the entire brain at 3rd DPI as compared to 14R-infected group. There were no significant differences observed between EHV-9- and 19R-infected groups (Fig. 7). Control hamsters euthanized showed no viral-associated brain histopathology throughout the experiment.

### *Topographical localization of viral antigens by immunohistochemistry*

Topographically, viral antigen-positive neurons were mostly associated with the histopathological lesions with antigens localized primarily in the neuronal body, processes and neuropil (Fig. 8). Viral antigens were also detected in the mitral and tufted layers of the olfactory lobes at 3rd DPI in both EHV-9- and 19R-infected groups. Moreover, viral antigens increased at 4th DPI in the above-mentioned groups and grew more abundant by 5th DPI. On the other hand, no viral antigens were detected in the olfactory bulb at

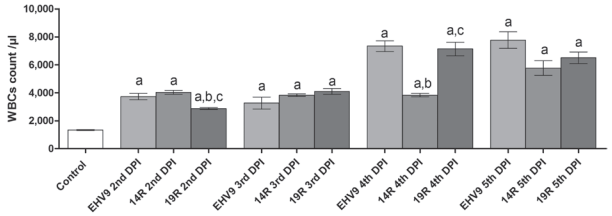


**Fig. 2.** Changes of WBCs count. Significant differences were observed in the control (a), EHV-9 -infected (b) and 14R-infected (c) groups. $P \leq 0.05$.

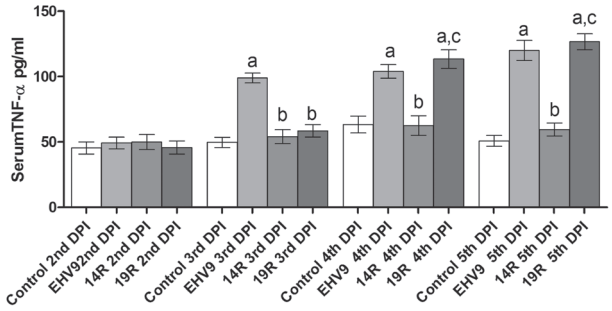


**Fig. 3.** Enzyme-linked immunosorbent assay (ELISA) for detecting serum TNF-α levels (*p*g/m*l*) in hamsters infected with EHV-9, 14R or 19R over 5 DPI. Significant differences were observed from the control (a), EHV-9 -infected (b) and 14R-infected (c) groups. Data analysis was performed separately for each day (n=5). $P \leq 0.05$.

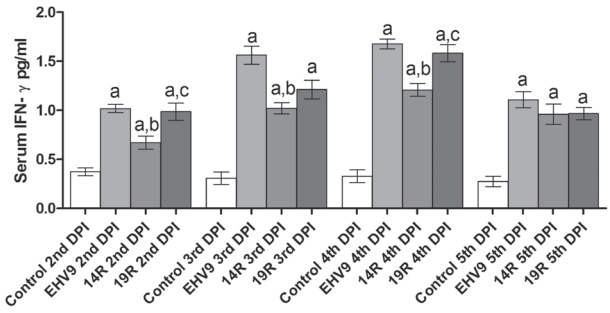


**Fig. 4.** Enzyme-linked immunosorbent assay for detecting serum IFN-γ levels (*p*g/m*l*) in hamsters infected with EHV-9, 14R or 19R over 5 DPI. Significant differences were observed from the control (a), EHV-9-infected (b) or 14R-infected (c) group. Data analysis was performed separately for each day (n=5). $P \leq 0.05$.

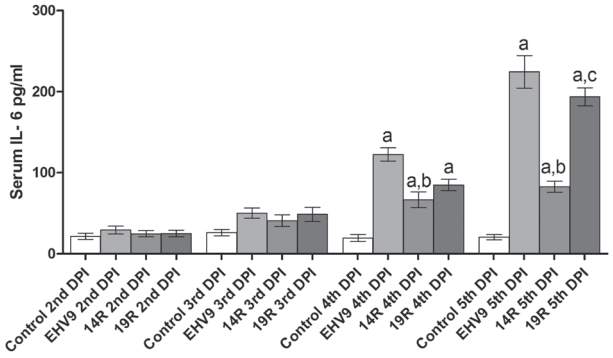


**Fig. 5.** Enzyme-linked immunosorbent assay for detecting serum IL-6 levels (*p*g/m*l*) in hamsters infected with EHV-9, 14R or 19R over 5 DPI. Significant differences were observed from the control group (a), the EHV9-infected group (b) or the 14R-infected group (c). Data analysis was performed separately for each day (n=5). $P \leq 0.05$.

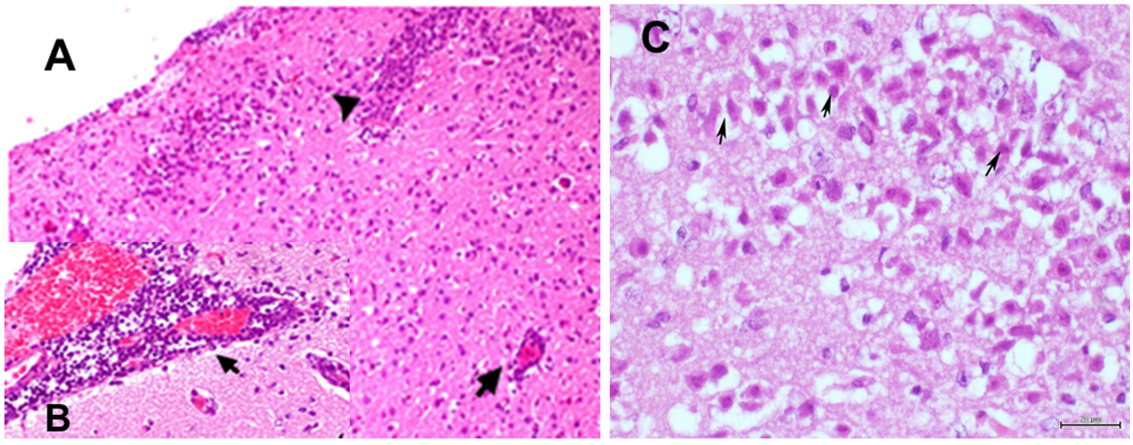


**Fig. 6.** Non-suppurative meningoencephalitis in hamsters infected with EHV-9, 19R or 14R in the form of (A), focal gliosis in the brain cortex (arrowhead), H&E, Bar=100 $\mu$m with perivascular cuffing (arrows). The inset picture (B) shows higher magnification of perivascular cuffing. (C) Neuronal degeneration and necrosis with nuclear shrinkage and vacuolation (arrows). H&E, Bar=100 $\mu$m.

3rd DPI in 14R-infected hamsters, and only a small amount of EHV-9 antigen was found at 4th and 5th DPI (Fig. 9). No positive immunostaining was observed in the olfactory bulb at 2nd DPI in all infected groups.

On the 4th DPI, the immunolabeling increased and was widely distributed within the cerebral cortex, limbic system and medulla oblongata in EHV-9- and 19R-infected groups (Fig. 10A–D). Mild positive immunostaining was observed at 4th and 5th DPI in cerebral cortex in 14R-infected animals, whereas no positive immunostaining was detected in the medulla oblongata at either time point (Fig. 10E and 10F).

The intensity of positive immunostaining was significantly higher in EHV-9- and 19R-infected groups than in the 14R-infected group at all time points starting from 3rd DPI (Fig.7). The cerebellum and spinal cords were negative for viral antigens at all time points.

## DISCUSSION

The observed differences in the onset and severity of clinical signs between both EHV-9- and 19R- infected groups compared to 14R-infected group may be a result of the different gene products between the parent virus (EHV-9) and its mutant (14R) which resulted from the point mutation in ORF19, so this resulted in difference in the neuropathogenecity as explained in herpes simplex virus type 1 (HSV-1) and other herpes viruses as the gene product of UL41 (ORF19), virion host shutoff (vhs) protein, plays a role in the neurotropism of this virus [27].

The decreased bodyweight gain in both EHV-9- and 19R-infected groups compared to 14R-infected group was also an important indicator for these clinical differences, which mainly resulted from in appetence and dehydration in both infected groups. Moreover, the decreases in bodyweight gain due to the EHV-9 infection were consistent with previous reports [10, 12, 33, 34].

Hematological analysis revealed a significant increase in WBCs in response to viral infection, consistent with previous reports [33]; however, the significant increase in the total WBCs in both EHV-9- and 19R-infected groups compared to the 14R-infected group at 4th DPI, highlights the low virulence of 14R that may attributed to the effect of the point mutation in this virus. In addition, both EHV-9- and 19R viral antigens were detected earlier in blood samples as compared to that in 14R-infected hamsters, consistent with the time of onset of clinical signs. This finding further supported the delayed virulence of the 14R mutant, and this delayed viremia was mainly due to one point mutation as it was previously reported that mutation in EHV-1 affects the virulence of the virus and had a significant effect on the overall level of viremia [14]. The onset of viremia of the virulent virus (EHV-9) is consistent with the previous report [15].

Previous reports on EHV-9 neuropathogenesis after intranasal inoculation demonstrated that the virus replicated in olfactory mucosal cells, entered the brain via the olfactory nerve and then spread trans-synaptically to connecting neurons along the olfactory tract, and subsequently replicated in olfactory bulb neurons, cerebrum and mesencephalon [12, 22]. Therefore, we compared the transmission of EHV-9, 19R and 14R virions in different parts of the brain by PCR. These results revealed that the 14R mutant exhibited delayed progression inside the brain relative to EHV-9- and 19R. This delayed progress might explain the fact that 14R-infected group had showed clinical signs later than both EHV-9- and 19R-infected groups.

Many gene products are essential for the anterograde transmission of herpes viruses. In the case of pseudorabies virus, mutations in Us9 interfere with the anterograde virus transmission in the axon [26]; thus, we can attribute the delayed progress of 14R in the brain tissue to the ORF19 point mutation that resulted in different gene products.

Cytokines are small glycoproteins produced by various cell types, primarily leukocytes, and regulate innate immunity, acquired immunity and a plethora of inflammatory responses [17]. In this study, we examined TNF-α, IFN-γ and IL-6 in the serum of control and infected hamsters. Since local increases in TNF-α induce heat, swelling, redness and inflammation [17], we hypothesized that the non-significant changes in TNF-α in the 14R-infected group might be a result of the point mutation in ORF19, leading to decreased and delayed signs of encephalitis. On the other hand, the increased TNF-α may hinder bodyweight gain in both EHV-9- and 19-R-infected animals and could be attributed to its effect on hypothalamic regulatory regions of the brain as an endogenous pyrogen induces fever and suppresses appetite [17].

The early host defense against an infection is likely to utilize IFN-γ secreted by NK and antigen-presenting cells [17]. In the present study, IFN-γ levels were significantly higher at all time points in all infected groups compared to controls as a protective immune response, consistent with previous reports on EHV-1 infection in non-vaccinated ponies [5]. Both IFN-γ and TNF- α can have a direct effect on brain tissue, and IFN-γ augments TNF-α synthesis, and both might mediate many aspects of the disease [3, 17]. Both TNF-α and IFN-γ are directly toxic to oligodendrocytes [21, 32], and similarly with other cytokines, can also stimulate local production of inflammatory cytokines [19]. In addition, the present results revealed that IFN-γ was significantly increased in both EHV-9- and 19R-infected group compared to 14R-infected group at 2nd and 4th DPI, suggesting that the low IFN-γ production may result from the point mutation in ORF 19.

IL-6 plays an important role in initiating and maintaining inflammatory responses during infection and in autoimmune disease [16]. Its expression is affected in many brain diseases and animal models, which strongly suggests that IL-6 could have a neuropathological role since its expression increases following axonal damage in neurons [11]. Therefore, the low levels of serum IL-6 in the 14R-infected animals compared to the EHV-9- and 19R-infected animals at 5th DPI may be due to a mild degree of brain injury that may be attributed to the effect of the point mutation in this mutant, which was confirmed by histopathological results as discussed below. It is interesting to note that HSV infection can act as a potent inducer of IL-6, which is further augmented in the presence of IFN-γ [24]. IL-6 can also be synthesized by mononuclear phagocytes, vascular endothelial cells, fibroblasts and other cells in response to trauma, burns, tissue damage, inflammation and TNF-α [17], which may explain the

**Table 5.** Histopathological changes and IHC Scoring for detection of viral antigen from brain samples of hamster groups infected with EHV-9, 19R or 14R during the course of intranasal infection

| DPI | No. | EHV-9 infected group | | | | | | 19R infected group | | | | | | 14R infected group | | | | | |
|---|---|---|---|---|---|---|---|---|---|---|---|---|---|---|---|---|---|---|---|
| | | Olfactory bulb | | Cerebrum | | Brain stem | | Olfactory bulb | | Cerebrum | | Brain stem | | Olfactory bulb | | Cerebrum | | Brain stem | |
| | | Histo | IHC | Histo | IHC | Histo | IHC | Histo | IHC | Histo | IHC | Histo | IHC | Histo | IHC | Histo | IHC | Histo | IHC |
| 2nd DPI | 1 | 0 | – | 0 | – | 0 | – | 0 | – | 0 | – | 0 | – | 0 | – | 0 | – | 0 | – |
| | 2 | 0 | – | 0 | – | 0 | – | 0 | – | 0 | – | 0 | – | 0 | – | 0 | – | 0 | – |
| | 3 | 0 | – | 0 | – | 0 | – | 0 | – | 0 | – | 0 | – | 0 | – | 0 | – | 0 | – |
| | 4 | 0 | – | 0 | – | 0 | – | 0 | – | 0 | – | 0 | – | 0 | – | 0 | – | 0 | – |
| | 5 | 0 | – | 0 | – | 0 | – | 0 | – | 0 | – | 0 | – | 0 | – | 0 | – | 0 | – |
| 3rd DPI | 1 | 3 | ++ | 2 | + | 0 | – | 2 | + | 1 | + | 0 | + | 0 | – | 0 | – | 0 | – |
| | 2 | 2 | + | 2 | + | 0 | – | 3 | + | 1 | + | 0 | – | 0 | – | 0 | – | 0 | – |
| | 3 | 2 | + | 2 | + | 0 | – | 2 | + | 1 | + | 0 | + | 0 | – | 0 | – | 0 | – |
| | 4 | 3 | ++ | 2 | + | 0 | – | 3 | + | 1 | + | 1 | + | 0 | – | 0 | – | 0 | – |
| | 5 | 3 | ++ | 2 | + | 0 | – | 2 | + | 0 | + | 0 | – | 0 | – | 0 | – | 0 | – |
| 4th DPI | 1 | 4 | ++ | 4 | ++ | 1 | + | 3 | ++ | 3 | ++ | 1 | + | 0 | – | 0 | – | 0 | – |
| | 2 | 4 | ++ | 3 | ++ | 1 | + | 3 | ++ | 3 | ++ | 0 | + | 0 | – | 0 | – | 0 | – |
| | 3 | 3 | ++ | 2 | ++ | 0 | + | 3 | ++ | 3 | ++ | 1 | + | 0 | – | 0 | – | 0 | – |
| | 4 | 3 | ++ | 3 | ++ | 0 | + | 3 | ++ | 2 | ++ | 1 | + | 1 | + | 0 | – | 0 | – |
| | 5 | 4 | ++ | 3 | ++ | 1 | + | 3 | ++ | 2 | ++ | 1 | + | 0 | – | 0 | – | 0 | – |
| 5th DPI | 1 | 4 | +++ | 4 | +++ | 2 | + | 3 | +++ | 3 | +++ | 1 | + | 0 | – | 0 | – | 0 | – |
| | 2 | 4 | +++ | 4 | +++ | 1 | ++ | 3 | +++ | 3 | ++ | 1 | + | 0 | – | 0 | – | 0 | – |
| | 3 | 3 | +++ | 3 | +++ | 1 | + | 4 | +++ | 3 | +++ | 1 | + | 2 | ++ | 1 | ++ | 0 | – |
| | 4 | 4 | +++ | 3 | +++ | 1 | + | 4 | +++ | 3 | ++ | 1 | + | 0 | – | 0 | – | 0 | – |
| | 5 | 4 | +++ | 4 | +++ | 2 | ++ | 3 | +++ | 3 | +++ | 1 | + | 1 | + | 1 | – | 0 | – |

Histo=Histopathological Changes., 0, no lesions; 1, minimal; 2, mild; 3, moderate; 4, severe., (−) Negative, (+), (++) and (+++) positive.

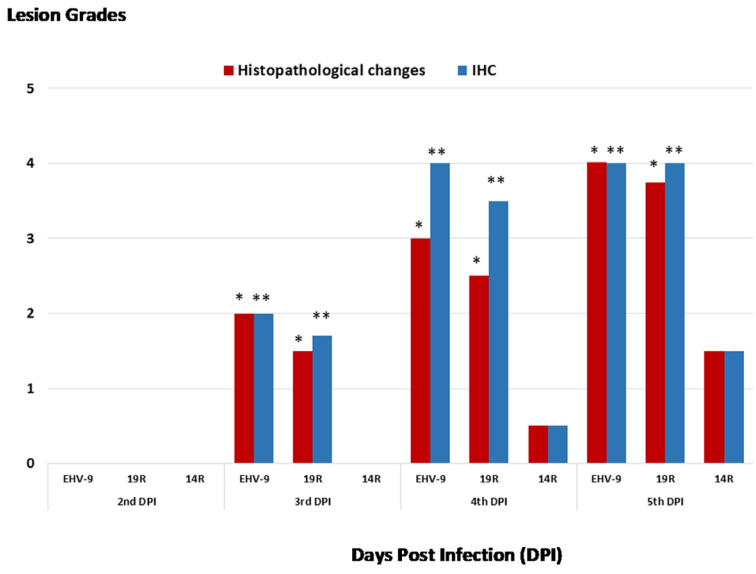


**Fig. 7.** Mean histopathological scores and immunohistochemical labeling for the entire brain at various time points of hamsters infected with EHV-9, 19R or 14R. * and ** indicate significant differences from the 14R-infected hamsters at the same time points ($P \leq 0.05$). Vertical axis indicates lesion grades.

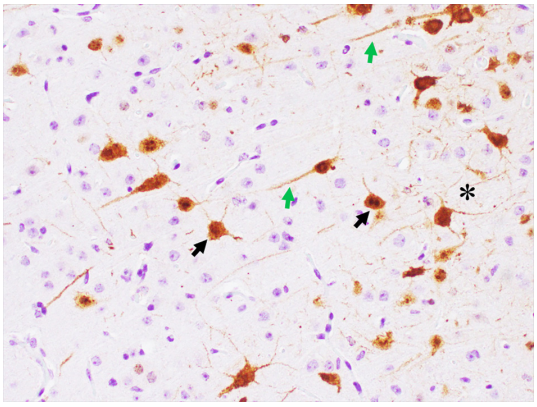

**Fig. 8.** Immunohistochemistry for viral distribution in the brain. Viral antigens were localized in the neuronal body (black arrows), processes (green arrows) and neuropil (star shape). Bar=50 $\mu$m.

synergistic effects seen between IL-6, INF-γ and TNF-α and their role in encephalitis.

The observed histopathological lesions were similar to those described in Thomson's gazelles naturally infected with EHV-9, as well as other animals experimentally infected with EHV-9, such as hamsters, goats, horses, pigs, dogs, cats and polar bears [6, 12, 13, 22, 30, 31, 33, 34]. Infected animals generally exhibit severe encephalitis characterized by perivascular cuffing, intranuclear inclusion bodies, neuronal degeneration and microglial activation. The distribution and severity of the encephalitic changes varied depending on the viral strain. Notably, the 14R virus did not induce encephalitis in all the infected animals, and the inflammatory

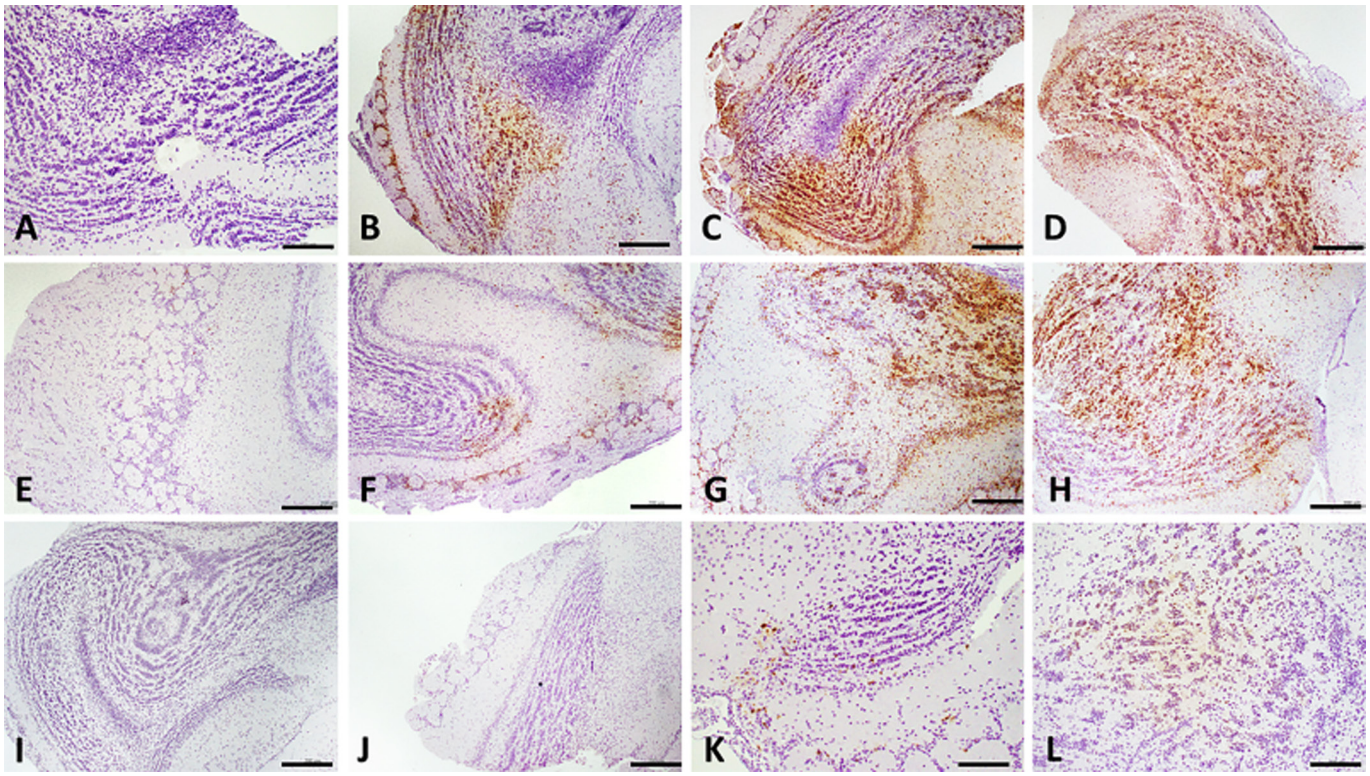


**Fig. 9.** Comparisons of viral antigens distribution in the olfactory bulb part of the 3 viral infected groups (EHV-9, 19R and 14R, respectively). A, B, C and D represent immunolabeled neurons (brown color) of olfactory bulb of hamsters inoculated with EHV-9 at (2nd DPI (A), 3rd DPI (B), 4th DPI (C) and 5th DPI (D), respectively). E, F, G and H represent immunolabeled neurons (brown color) of olfactory bulb of hamsters inoculated with 19R at (2nd DPI (E), 3rd DPI (F), 4th DPI (G) and 5th DPI (H), respectively). I, J, K and L represent immunolabeled neurons (brown color) of olfactory bulb of hamsters inoculated with 14R at (2nd DPI (I), 3rd DPI (J), 4th DPI (K) and 5th DPI (L), respectively). IHC, Bar=100 $\mu$m.

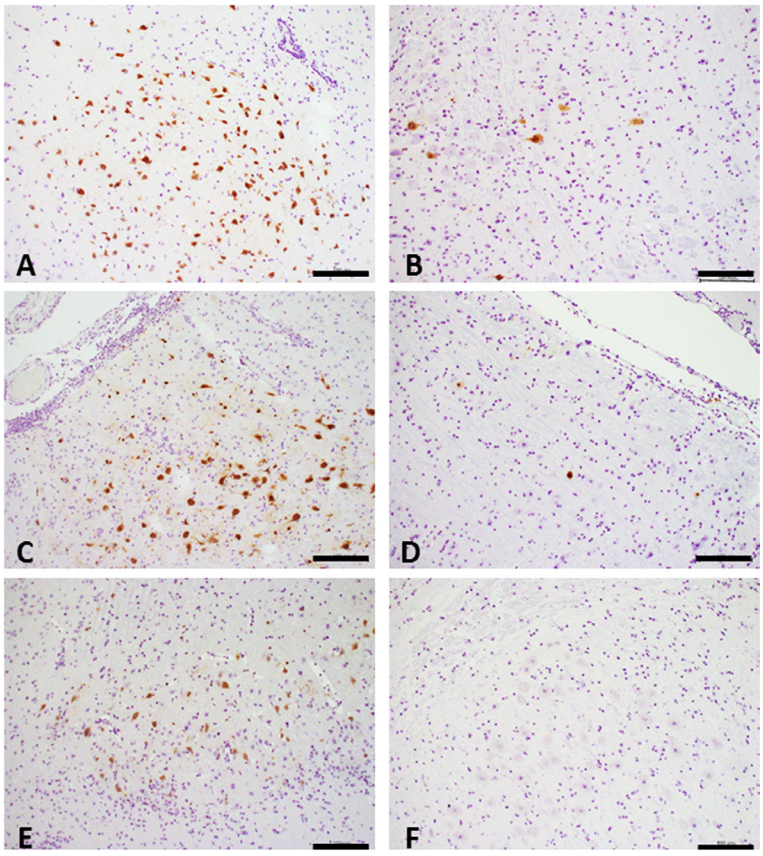


**Fig. 10.** Distribution of viral antigens (brown color) in the cerebrum of hamsters inoculated with EHV-9 (A and B), 19R (C and D) and 14 R (E and F) at 4th and 5th DPI. A, C and E (immunopositivity reaction in frontal cortex). B, D and F (immunopositivity reaction in medulla oblongata). IHC, Bar=50 $\mu$m.

changes, when present, showed the same distribution as that in animals infected with EHV-9 or 19R. The olfactory bulbs of the hamsters were the most severely affected portion of the brain. It was previously hypothesized that a possible infection route for EHV-9 begins at the nasal mucosa and along the olfactory pathway [8], and extends from the olfactory bulb to the rhinencephalon and piriform lobe. The lesions then spread to the basal ganglia and the limbic lobe, including the hippocampus, cingulate gyrus, basal forebrain and temporal lobe. Besides a mild lesion in the midbrain and medulla oblongata, we observed widely distributed lesions in the cerebrum of infected hamsters that were euthanized at 5th DPI. No other abnormalities were observed in the cerebellum or spinal cord, which was consistent with previous studies [12, 18].

Our histopathological analysis revealed that mean group scores for the entire brain were significantly higher in hamsters inoculated with EHV-9 or 19R than for those inoculated with 14R at all time points starting from 3rd DPI. In contrast, no significant differences were observed between EHV-9- and 19R at all time points. Moreover, 14R-infected animals showed minimal and slower development of the pathological lesions, suggesting that the point mutation in ORF19 was responsible for the observed low virulence.

Immunohistochemistry revealed the presence of EHV-9 antigen in neurons and neuronal fibers, including the axons and dendrites. These findings indicate a trans-synaptic spread of EHV-9 from neuron to neuron via the neuronal fibers in the brain, as shown in pseudorabies infections [28]. The pattern of immunostaining was consistent with previous studies [7, 8]. Moreover, the IHC scores were significantly higher in both EHV-9 and 19R-infected groups than in 14R at all time points starting from 3rd DPI.

In conclusion, the observed clinical observations, hematological changes, viremia, PCR on brain tissue and inflammatory cytokines together with immunohistopathological analysis of the brain confirm that mutation in ORF 19 is responsible for the attenuation of EHV-9. Therefore, ORF19 plays an important role in the pathogenesis of EHV-9. Further studies are necessary to detect additional genes that contribute to the pathogenesis of EHV-9, which enable us to control the infection with virus by using a suitable vaccine.

ACKNOWLEDGMENTS. This study was supported in part by a grant-in-aid for scientific research from the Ministry of Health, Labor, and Welfare of Japan and grants from Hokkaido University and Ono Pharmaceutical Co., Ltd. The authors acknowledge staff members of the Pathology and Microbiology Department of Gifu University, and the Animal Medicine Department of Damanhour University.

## REFERENCES

1. Angsubhakorn, S., Moe, J. B., Latendresse, J. R., Ward, G. S., Ngamprochana, M., Sahaphong, S. and Bhamarapravati, N. 1986. The neurovirulence of flaviviruses in crab-eating monkeys (Macaca fascicularis). *Southeast Asian J. Trop. Med. Public Health* **17**: 604–612. [Medline]
2. Anwar, S., Yanai, T. and Sakai, H. 2015. Immunohistochemical detection of urokinase plasminogen activator and urokinase plasminogen activator receptor in canine vascular endothelial tumours. *J. Comp. Pathol.* **153**: 278–282. [Medline] [CrossRef]
3. Bettelli, E. and Nicholson, L. B. 2001. The role of cytokines in experimental autoimmune encephalomyelitis. pp. 109–127. *In*: Autoimmunity, Springer, New York.
4. Borchers, K., Wiik, H., Frölich, K., Ludwig, H. and East, M. L. 2005. Antibodies against equine herpesviruses and equine arteritis virus in Burchell's zebras (Equus burchelli ) from the Serengeti ecosystem. *J. Wildl. Dis.* **41**: 80–86. [Medline] [CrossRef]
5. Coombs, D. K., Patton, T., Kohler, A. K., Soboll, G., Breathnach, C., Townsend, H. G. and Lunn, D. P. 2006. Cytokine responses to EHV-1 infection in immune and non-immune ponies. *Vet. Immunol. Immunopathol.* **111**: 109–116. [Medline] [CrossRef]
6. Donovan, T. A., Schrenzel, M. D., Tucker, T., Pessier, A. P., Bicknese, B., Busch, M. D., Wise, A. G., Maes, R., Kiupel, M., McKnight, C. and Nordhausen, R. W. 2009. Meningoencephalitis in a polar bear caused by equine herpesvirus 9 (EHV-9). *Vet. Pathol.* **46**: 1138–1143. [Medline] [CrossRef]
7. El-Habashi, N., Kato, Y., El-Nahass, E., Fukushi, H., Hirata, A., Sakai, H., Kimura, J. and Yanai, T. 2013. An ocular infection model using suckling hamsters inoculated with equine herpesvirus 9 (EHV-9): kinetics of the virus and time-course pathogenesis of EHV-9-induced encephalitis via the eyes. *Vet. Pathol.* **50**: 56–64. [Medline] [CrossRef]
8. El-Habashi, N., Murakami, M., El-Nahass, E., Hibi, D., Sakai, H., Fukushi, H., Sasseville, V. and Yanai, T. 2011. Study on the infectivity of equine herpesvirus 9 (EHV-9) by different routes of inoculation in hamsters. *Vet. Pathol.* **48**: 558–564. [Medline] [CrossRef]
9. El-Habashi, N., El-Nahass, E.S., Namihira, Y., Hagiwara, H., Fukushi, H., Narita, M., Hirata, A., Sakai, H. and Yanai, T. 2011. Neuropathogenicity of equine herpesvirus 9 in cattle. *J. Equine Vet. Sci.* **31**: 72–77. [CrossRef]
10. El-Nahass, E., El-Habashi, N., Nayel, M., Kasem, S., Fukushi, H., Suzuki, Y., Hirata, A., Sakai, H. and Yanai, T. 2011. Kinetics and pathogenicity of equine herpesvirus-9 infection following intraperitoneal inoculation in hamsters. *J. Comp. Pathol.* **145**: 271–281. [Medline] [CrossRef]
11. Erta, M., Quintana, A. and Hidalgo, J. 2012. Interleukin-6, a major cytokine in the central nervous system. *Int. J. Biol. Sci.* **8**: 1254–1266. [Medline] [CrossRef]
12. Fukushi, H., Taniguchi, A., Yasuda, K., Yanai, T., Masegi, T., Yamaguchi, T. and Hirai, K. 2000. A hamster model of equine herpesvirus 9 induced encephalitis. *J. Neurovirol.* **6**: 314–319. [Medline] [CrossRef]
13. Fukushi, H., Tomita, T., Taniguchi, A., Ochiai, Y., Kirisawa, R., Matsumura, T., Yanai, T., Masegi, T., Yamaguchi, T. and Hirai, K. 1997. Gazelle herpesvirus 1: a new neurotropic herpesvirus immunologically related to equine herpesvirus 1. *Virology* **227**: 34–44. [Medline] [CrossRef]
14. Goodman, L. B., Loregian, A., Perkins, G. A., Nugent, J., Buckles, E. L., Mercorelli, B., Kydd, J. H., Palù, G., Smith, K. C., Osterrieder, N. and Davis-Poynter, N. 2007. A point mutation in a herpesvirus polymerase determines neuropathogenicity. *PLoS Pathog.* **3**: e160. [Medline] [CrossRef]
15. Hussey, G. S., Goehring, L. S., Lunn, D. P., Hussey, S. B., Huang, T., Osterrieder, N., Powell, C., Hand, J., Holz, C. and Slater, J. 2013. Experimental infection with equine herpesvirus type 1 (EHV-1) induces chorioretinal lesions. *Vet. Res. (Faisalabad)* **44**: 118. [Medline] [CrossRef]
16. Ishihara, K. and Hirano, T. 2002. IL-6 in autoimmune disease and chronic inflammatory proliferative disease. *Cytokine Growth Factor Rev.* **13**: 357–368. [Medline] [CrossRef]
17. Khan, M. M. 2008. Role of cytokines. pp. 33–59. *In*: Immunopharmacology, Springer US, Boston.

18. Kodama, A., Yanai, T., Yomemaru, K., Sakai, H., Masegi, T., Yamada, S., Fukushi, H., Kuraishi, T., Hattori, S. and Kai, C. 2007. Acute neuropathogenicity with experimental infection of equine herpesvirus 9 in common marmosets (Callithrix jacchus). *J. Med. Primatol.* **36**: 335–342. [Medline] [CrossRef]
19. Liu, J. S., Amaral, T. D., Brosnan, C. F. and Lee, S. C. 1998. IFNs are critical regulators of IL-1 receptor antagonist and IL-1 expression in human microglia. *J. Immunol.* **161**: 1989–1996. [Medline]
20. Maximova, O. A., Ward, J. M., Asher, D. M., St Claire, M., Finneyfrock, B. W., Speicher, J. M., Murphy, B. R. and Pletnev, A. G. 2008. Comparative neuropathogenesis and neurovirulence of attenuated flaviviruses in nonhuman primates. *J. Virol.* **82**: 5255–5268. [Medline] [CrossRef]
21. Merrill, J. E., Ignarro, L. J., Sherman, M. P., Melinek, J. and Lane, T. E. 1993. Microglial cell cytotoxicity of oligodendrocytes is mediated through nitric oxide. *J. Immunol.* **151**: 2132–2141. [Medline]
22. Narita, M., Uchimura, A., Kawanabe, M., Fukushi, H. and Hirai, K. 2001. Invasion and spread of equine herpesvirus 9 in the olfactory pathway of pigs after intranasal inoculation. *J. Comp. Pathol.* **124**: 265–272. [Medline] [CrossRef]
23. Nathanson, N., Goldblatt, D., Thind, I. S., Davis, M. and Price, W. H. 1965. Histological studies of the monkey neurovirulence of group B arboviruses. I. A semiquantitative grading scale. *Am. J. Epidemiol.* **82**: 359–381. [Medline] [CrossRef]
24. Paludan, S. R. 2001. Requirements for the induction of interleukin-6 by herpes simplex virus-infected leukocytes. *J. Virol.* **75**: 8008–8015. [Medline] [CrossRef]
25. Schrenzel, M. D., Tucker, T. A., Donovan, T. A., Busch, M. D., Wise, A. G., Maes, R. K. and Kiupel, M. 2008. New hosts for equine herpesvirus 9. *Emerg. Infect. Dis.* **14**: 1616–1619. [Medline] [CrossRef]
26. Smith, G. 2012. Herpesvirus transport to the nervous system and back again. *Annu. Rev. Microbiol.* **66**: 153–176. [Medline] [CrossRef]
27. Strelow, L. I. and Leib, D. A. 1995. Role of the virion host shutoff (vhs) of herpes simplex virus type 1 in latency and pathogenesis. *J. Virol.* **69**: 6779–6786. [Medline]
28. Takahashi, H., Kai, C., Yoshikawa, Y. and Yamanouchi, K. 1995. Immunohistochemical analysis of pseudorabies virus spread through neurons innervating the eyeball. *Comp. Immunol. Microbiol. Infect. Dis.* **18**: 275–281. [Medline] [CrossRef]
29. Tamura, T., Sakoda, Y., Yoshino, F., Nomura, T., Yamamoto, N., Sato, Y., Okamatsu, M., Ruggli, N. and Kida, H. 2012. Selection of classical swine fever virus with enhanced pathogenicity reveals synergistic virulence determinants in E2 and NS4B. *J. Virol.* **86**: 8602–8613. [Medline] [CrossRef]
30. Taniguchi, A., Fukushi, H., Matsumura, T., Yanai, T., Masegi, T. and Hirai, K. 2000. Pathogenicity of a new neurotropic equine herpesvirus 9 (gazelle herpesvirus 1) in horses. *J. Vet. Med. Sci.* **62**: 215–218. [Medline] [CrossRef]
31. Taniguchi, A., Fukushi, H., Yanai, T., Masegi, T., Yamaguchi, T. and Hirai, K. 2000. Equine herpesvirus 9 induced lethal encephalomyelitis in experimentally infected goats. *Arch. Virol.* **145**: 2619–2627. [Medline] [CrossRef]
32. Vartanian, T., Li, Y., Zhao, M. and Stefansson, K. 1995. Interferon-gamma-induced oligodendrocyte cell death: implications for the pathogenesis of multiple sclerosis. *Mol. Med.* **1**: 732–743. [Medline]
33. Yanai, T., Fujishima, N., Fukushi, H., Hirata, A., Sakai, H. and Masegi, T. 2003. Experimental infection of equine herpesvirus 9 in dogs. *Vet. Pathol.* **40**: 263–267. [Medline] [CrossRef]
34. Yanai, T., Tujioka, S., Sakai, H., Fukushi, H., Hirai, K. and Masegi, T. 2003. Experimental infection with equine herpesvirus 9 (EHV-9) in cats. *J. Comp. Pathol.* **128**: 113–118. [Medline] [CrossRef]
35. Yanai, T., Kodama, A., Kai, C., Fukushi, H., Sakai, H., Hattori, S. and Kuraishi, T. 2011. Equine Herpesvirus 9 (EHV-9) Induced Encephalitis in Nonhuman Primates. Intech Open Access Publisher.
36. Yanai, T., Sakai, T., Fukushi, H., Hirai, K., Narita, M., Sakai, H. and Masegi, T. 1998. Neuropathological study of gazelle herpesvirus 1 (equine herpesvirus 9) infection in Thomson's gazelles (Gazella thomsoni). *J. Comp. Pathol.* **119**: 159–168. [Medline] [CrossRef]